Title: Spectroscopical and Computational investigation on Pharmacological activity on the structure of 1-Benzylimidazole

Authors: A. Madanagopal, S. Periandy, P. Gayathri, S. Ramalingam, S. Xavier, vladimir K. Ivanov

PII: S1658-3655(17)30029-8
DOI: http://dx.doi.org/doi:10.1016/j.jtusci.2017.02.006
Reference: JTUSCI 366

To appear in:

Received date: 5-11-2016
Accepted date: 18-2-2017

Please cite this article as: A.Madanagopal, S.Periandy, P.Gayathri, S.Ramalingam, S.Xavier, vladimir K.Ivanov, Spectroscopical and Computational investigation on Pharmacological activity on the structure of 1-Benzylimidazole (2010), http://dx.doi.org/10.1016/j.jtusci.2017.02.006

Spectroscopical and Computational investigation on Pharmacological activity on the structure of 1-Benzylimidazole

A. Madanagopal[a], S. Periandy[b], P. Gayathri[a], S. Ramalingam[c], S. Xavier[d], vladimir K. Ivanov[e]

[a] Department of Physics, Periyar Maniammai University, Thanjavur, Tamilnadu, India.

[b]Department of Physics, Kanchi Mamunivar Centre for PG studies, Puducherry, India.

[c] PG and Research department of Physics, A.V.C. College, Mayiladuthurai, Tamilnadu, India.

[d]Department of Physics, St. Joseph College of Arts and Science, Cuddalore, Tamil Nadu, India.

[e] Kurnakov Institute of General and Inorganic Chemistry, 31 Leninsky avenue Moscow 119991 Russia.

**Corresponding author: ramalingam.physics@gmail.com*

Tel./Fax: +91 04364 225367

ABSTRACT

The chemical and pharmacological activity of the compound; 1-benzylimidazole has been interpreted using vibrational, NMR and UV-Visible spectroscopic tools. The necessary data obtained by recording spectra of FT-IR, FT-Raman, NMR and UV-Visible. ^{1}H and ^{13}C NMR spectral chemical shift have been observed and investigated for the interpretation of origin of the antiparasitic, antifungal and antimicrobial activities. The elaborate electronic excitational absorptions are keenly noted where in which bathochromic shift in the UV-Visible spectrum for the cause of the strong cardio tonic activity. The pharmacodynamic activity related to the molecular polarization analyzed from different analytical parameters. The molecular reactivity is studied from the dislocation of charge levels in Frontier molecular orbitals. NBO analysis is carried out to picture the asymmetric charge interactional transitions among the orbitals on par with the pharmacological behavior of the compound. The enantiomer errors in the electronic structure have been analyzed by simulating ECD and VCD spectra.

Keywords:1-benzylimdazole, pharmacological, FT-IR, FT-Raman, NMR, cardio tonic activity, enantiomer, ECD and VCD spectra.

1. Introduction

The Benzylimidazole [1] is heterocyclic aromatic compound with a benzene ring fused with imidazole through ethylene group. Benzylimidazole is used as a procarcinogenic or mutagenic compound. It is the extension of imidazole system which is used as skeleton for N-heterocyclic carbons. Benzylimidazole is found to induce various cytochromes P-450 (CYP) isozymes. The compound has been found to decrease the plasma triglyceride levels and as a potent inducer of rat liver enzymes. Benzylimidazole stimulates three distinct forms of UDP-glucuronosyltransferase. In addition, Benzylimidazole also inhibit TXA Synthase (thromboxane A_2 synthase) and has a strong cardio tonic activity similar to the cardiac glycosides, including the absence of effects on rate and resistance to adrenergic beta blockers. N-substituted derivatives of imidazole and Benzylimidazole are also a subject of interest to organic and medicinal chemists

because they exhibit variety pharmacological properties, such as antiparasitic [2], antifungal [3], and antimicrobial activities [4].These compounds were investigated for antibacterial activity against Escherichia Coli, Staphylococcus aureus and Pseudomanasaureginosa [5]. It has been reported that the length of the alkyl chain on the imidazole ring is of importance for biological activity; antifungal and cytotoxic activity for inhibition of microsomal oxidation [6].

Hofmanm [7] has studied the molecule and reported that, the imidazole ring is the basic chemical structure for a number of pharmacologically active substances, including the imidazolines which have both adrenergic *alpha* receptor stimulant, the G-protein coupled receptor combining catecholamine which stimulates sympathetic nervous system responsible for fight or flight response in human body. In a recent paper, Knopeet al. [8] reported that imidazole possess positive isotropic which affects the force of heart muscle contraction, but not chronoscopic which increases the heart rate by affecting the force of heart contracting muscle. The intropism was not blocked by propranolol. Recent studies by Vermaand McNeil [9] also show that unlike the catecholamine's, imidazole does not increase cyclic 3',S'-adenosine mono phosphate. These data indicate that, the imidazoles, like the cardiac glycosides and Ca^{++} may have actions unrelated to the catecholamines.

The literature survey disclosed that, combined ^{1}H and ^{13}C NMR and UV-Visible studies supported by quantum computational tool have not been reported so far on 1-Benzylimidazole in spite of its wide-ranging biological applications. Hence, a detailed the vibrational pattern evidence for the active presence of organic compositions of the molecule is carried out in the present work. To know the multi phase biological reactive center, the detailed chemical shift investigation has been carried out. The rate of change of Mullikan charge levels according to the favor of orientation of molecular orbitals have been detailed illustrated with suitable diagram.

2. Experimental details

- The FT-IR spectrum of the compound was recorded using a Bruker IFS 66V spectrometer.

- The FT-Raman spectrum of the same compound was also recorded using the same instrument with an FRA 106 Raman module equipped with aNd:YAG laser source operating at 1.064 µm line widths with 200 mW power.
- The high resolution HNMR and CNMR spectra were recorded using 300 MHz and 75 MHz NMR spectrometer respectively.
- The UV-Vis spectra were recorded in liquid phase dissolved in ethanol in the range of 200 nm to 800 nm, with the scanning interval of 0.2 nm, using the UV-1700 series instrument.

3. Computational profile

The entire quantum chemical computations are performed using the Gaussian 09 D 01 version software program in core i7 computer [11]. The wave numbers and geometrical parameters are computed using B3LYP and B3PW91 methods in combination with 6-31++G(d, p) and 6-311++G(d,p) basis sets. The electronic spectra and related properties, such as NBO and HOMO-LUMO were calculated using time-dependent SCF method with same basis set. Similarly the ^{1}H and ^{13}CNMR chemical shifts are also carried out by GIAO method in combination with B3LYP/6-311++G(2d,p). The Mullikan charge distribution over the entire molecular orbitals is mapped and the values are deeply analyzed for the interpretation of the pharmaceutical application of the compound. The dipole moment, linear polarizability and the first order hyper polarizability of the compound are also computed using B3LYP method with the 6-311++G (d, p) basis set. The ECD and VCD spectra are simulated using same method and basis set.

4. Results and discussion

4.1. Conformational analysis

The molecular geometry scan is performed and the optimized geometry of the compound is identified by the zero point vibrational energy. The conformational analysis was performed by varying the torsion angle C1-C2-C12-N15 in the steps of 36º over one complete rotation 0-360° as recommended in the previous work on a similar compound [7]. It is also confirmed that, two

conformational structures (144º and the other at 324º with total energy 0.09486 and 0.09487hartree) have been found for the compound and is presented in Figure 1. The angle of substitution is periodic and non-symmetric by 180° since C1-C2 is exactly equivalent to C3-C2. The complete physico-chemical properties are explored in those two stable conformational structures.

4.2. Structural Deformation analysis

In this compound, the base molecule is benzene and is substituted by imidazole via ethylene group. The substitution; imidazole has strong imine group which is the main reason for the active pharmaceutical properties of the compound. Normally, the C-C bond lengths in hexagonal ring are sequentially arranged in regular manner, due to the mass of the substitution, the bond lengths are varied. Here, the ethyl group with imidazole ring is injected in ortho position of the ring. Proportionately, C1-C2 and C2-C3 bond lengths at the position of the substitution are expanded by 0.031Å and 0.019Å (Expt.) respectively. In order to sustain the substitution, the bond lengths C1-C2, C2-C3 and C5-C6 are stretched more than rest of others. In general, if the bond length of the benzene ring is changed much by the substitutions, the property of the ring will be changed on par with the substitutions [8]. Accordingly, here the benzene property is altered with respect to the imidazole and ethyl groups.

In imidazole ring, the hetero bond length N15-C16 is 0.012Å stretched than N15-C17 due to the holding of the entire ring. Among the C-N bonds within the imidazole group, bond length values of N15-C16, 22N-C18 and N15- C17 and are 1.38, 1.37 and 1.36 Å calculated by B3LYP and 1.37Å, 1.37Å and 1.36 Å by B3PW91 are closer to the experimental values 1.37Å, 1.37Å and 1.34Å respectively [9-10]. The bond length of imine group C17-N22 is 0.067Å shorter than the N15-C16 due to strong π orbital interaction (SP^3). Such type of alternating hetero-atoms bonds in the ring along with the phenyl ring may be related to the rich antifungal and antimicrobial activities in the compound. Such type of alternative hetero bonds in the ring along with the phenyl ring making the rich antifungal and antimicrobial activities in the compound. The interaction of C12 on H13 and H14 is higher than C on H of the benzene ring due to the

strong symmetrical holding of ethyl group which is acting as main root to transfer the imidazole ring property to the benzene ring.

4.3. Mulliken charge population analysis

The Mulliken charge delocalization is anisotropic since the partitioning of molecular orbitals depends on the strong directed bonds exist in the compound. The donation and back donation of electron density depends upon the generation of the enhanced bonds in the formation of the compound [11]. Normally, after the formation of the compound, the entire charge distribution is rearranged with respect to the existence of interactive (directed bonds) and repulsive bonds (weak bonds) in the compound. The home orbitals of the positive and negative atoms making the consecutive bonds of the molecule and thus the delocalized molecular orbitals in different bonds emphasize the rate change of chemical property of the compound.

The Mulliken charge levels of the title compound presented in the Table 2 and the color region in terms of the distribution of charge levels shown in the Figure 2 and 3. In this case, the entire C of the phenyl ring found to be moderate negative which is lower than the N15 and N22 in the imidazole ring. If the phenyl ring existed alone, the negative charge level of the ring C will be high. But here due to the substitutions, the negative charge level is partitioned i.e. electron clouds moved away from the phenyl ring. In addition to that, C12 and C18 are identified as more negative when compared to C16 which is mainly due to the dislocation of negative charges for the enrichment of the directed bond(C=N). The Mulliken charge population is moved from the benzene ring to the imidazole ring. So the physicochemical property is altered on par with the pentagonal ring. Thus, the asymmetrical delocalization of the charge levels for the formation of C=N and C-N in imidazole ring emphasize the 1-Benzylimidazole being antiparasitic, antifungal and antimicrobial compound.

4.4. Vibrational analysis

The fundamental active vibrational frequencies for 1-benzylimidazole are presented in Table. 2. The experimental and calculated FT-IR and FT-Raman vibrational spectra are displayed in the Figures 4 and 5 respectively. Two main ring and ethyl group of the compound

are composed by 22 atoms and the confinement belongs to C_S point group, hence CS point group is valid only for planar conformers. The 60 fundamental modes of vibrations are displayed as **Γ_{vib} = 40A′ + 20 A″.**

The entire quantum mechanical method and density force fields calculations are performed by combining the experimental and theoretical aspects of Pulay and Rauhut. Their training set and test set have been used to check the reliability of fitting. The overall scaling factors for theoretical harmonic frequencies have been verified with least-square fits [12-13]. The calculated wave numbers at B3LYP/ 6-311+ G (d, p) above 1340 cm^{-1} scaled by the factor 0.81158 and blow 1340 $cm^{-1}$by the factor 0.8995. Similarly wavenumber calculated at B3PW91/ 6-31+G (d, p) above 1340 $cm^{-1}$are scaled by 0.8782 and blow 1340 cm^{-1} by 0.8148 and in the same way B3PW91/ 6-311+G (d, p) are scaled by the factors 0.8734 and 0.8148 respectively.

4.4.1. C–H Vibrations

Usually, the enriched vibrational pattern of the compound described all the vibrational bands active and thereby it is ensured that, the physical and chemical activity is energetic. Accordingly, the phenyl ring has five C-H bonds and five stretching to be observed. Normally, the C–H stretching vibrations of the phenyl ring are normally observed in the region 3100–3000 cm^{-1}[13-15] which shows their uniqueness of the skeletal vibrations. In the present compound, the stretching vibrations have been appeared with weak to medium intensity at 3100, 3095, 3090, 3080, 3070, 3060, 3050 and 3000 cm^{-1}. All these bands are observed from the top end to lower end of the expected region. The PED proved that, those bands are pure and the stretching vibrations have not influenced by the imidazole and ethylene group vibrations.

Similarly, the C–H in-plane ring bending vibrations for aromatic C-H occurs as strong to weak intensity bands in the region 1300–1000 cm^{-1}[16]. In this case, seven bending bands are observed at 1290, 1280, 1260, 1210, 1200, 1130, 1120 and 1090 cm^{-1}. Similarly, the C–H out of plane bending vibrations are expected in the region 1000–750 cm^{-1}[17]. These vibrations are found at 910, 850, 820, 780, 760, 740, 720 and 700 cm^{-1}. In the present case, the in bending modes are within the limit and found top end of the limit whereas three of the out of plane bending appeared well below the expected region which indicate that, the out of plane bending modes alone are affected much by C-N and C-C vibrations.

4.4.2. Ethylene group vibrations

The aliphatic C-H stretching bands are expected in the region 3000 - 2900 cm^{-1}[18-19]. In the present compound the vibrations of the vinyl group are observed at 2950 and 2900 cm^{-1}. Similarly, the in-plane and out of-plane deformations of such C-H bond are expected in the regions 1200–1100 cm^{-1} and 900–700 cm^{-1} respectively. Four bands due to in-plane and out-of-plane bending are observed at 1090 & 1080 $cm^{-1}$and 690 and 660 cm^{-1} respectively. These observations indicate that the stretching modes are safe whereas in-plane and out-of-plane bending vibrations are moved down from the expected region, because ethylene group acts as bridge between imidazole and phenyl ring and it is always affected by either sides of the groups vibrations.

4.4.3. Imidazole group vibrations

Generally, imidazoles have several bands of variable intensity in the region of 1660-1450cm^{-1} due to C=N and C=C stretching vibrations [20-21]. In this case, the imidazole part is substituted mono, in which the C=N and C=C stretching vibrations are observed with strong and medium intensity at 1640 and 1510 cm^{-1} respectively. According to the above literatures, the in plane and out of plane bending modes as C=N-C and C=C-N are expect to be observed in the region 1070-925 cm^{-1} and 445-355 cm^{-1} respectively. Here, those bending vibrational bands identified at 1080 and 340 cm^{-1} respectively. In the five membered ring, the C-N stretching peaks usually observed in the frequency region 1382-1266 cm^{-1}. Here, the C-N stretching peaks observed with strong intensity at 1460, 1440, 1430 and 1410 cm^{-1}. The in plane and out of plane bending modes are found at 1050, 1040 and 1020 cm^{-1} and 340 and 250 cm^{-1} respectively. The stretching vibrations are moved up little beyond the expected region whereas the in plane bending vibrational peaks are climb arbitrarily due to the favoring of other suppressed bands. The frequency related to C-N bonds appeared in various places of the spectra since those bonds are appeared at two different parts of the compound. If the vibrational bands of substitutional group are very active, the chemical property of corresponding of the same will be intensive in the compound. In this case, very strong presence imidazole part vibrational wavenumbers emphasize its active presence.

4.4.4. CC vibrations

The CC stretching vibrations for phenyl ring are generally observed in the region of the spectrum 1600-1400 cm^{-1}[24-25], in which the bands between 1600-1500 cm^{-1} are assigned to C=C stretching and rest of others as C-C stretching. In the present compound, bands at 1620, 1620 and 1510 cm^{-1} are assigned to the phenyl ring C=C stretching vibrations and the peaks at 1380, 1350 and 1340 cm^{-1} assigned to C-C stretching modes. Generally, if the phenyl ring substituted, the corresponding ring vibrations will be set back some extent. This is true in this also that, the stretching related to π-CC bonds are moved up to the higher region whereas the stretching linked with σ-CC bonds moved down below the expected region of the spectrum. The C-C stretching, in pane and out of plane bending vibrations connected to out of the ring are observed at 1320, 920 and 150 cm^{-1} respectively. These vibrational modes are moved down due to the presence of intermediate place of the related bonds. The CCC in plane and out o the plane bending signals of the ring are found at 650, 610 and 590 cm^{-1} and 220 and 180 cm^{-1} respectively. As usually, these vibrational bands are get back from the lower limit of the permissible region. In five membered ring, the C-C-N in plane and out of plane bending vibrational frequencies are observed at 1010, 1000 and 990 cm^{-1} and 480 cm^{-1} respectively. Unlike the ring breathing of six membered ring, the ring bending vibrations are shifted up to higher region for the enhancement of the imidazole group.

4.5. NMR analysis

The paramagnetic shield of an atom described the chemical and physical property of the atom and whenever such shielding is broken by forming the bond with another atom and thereby the physicochemical property of the two atoms is changed with respect to the high degree of the electron cloud of the atom. Similarly, the molecule is formed by making bonds between the atoms and the corresponding chemical property of the product-compound is complicated and which depends upon the group of substitutional bonds and their asymmetrical displacement electron clouds [26]. Such type of electron cloud movement can be studied by the chemical shift of the associated atoms.

The computed values in gas and solvent phase, along with the experimental values are

presented in the Table 4 and the experimental spectra are presented in Figure 6. The aromatic carbon atoms generally [27] have shifts in the range of 120-130 ppm. In the present compound the chemical shifts of the aromatic ring carbon atoms except C2, namely C1, C3, C4, C5 and C6 are almost lie in the same range around 127ppm experimentally and between 133-134 ppm theoretically. In the case of C2, where the substitutional group is attached, the chemical shift is found to be 136 ppm experimentally and 146 ppm theoretically. This is purely due to the asymmetrical breaking of the paramagnetic shield of the particular carbon. Such a condition shows that, the inherent change of property of the benzene ring in this compound. This trend is in accordance with the charge predicted by Mullikan analysis.

The carbon atom C12 in the ethylene has chemical shift of 50 ppm experimentally and 53 ppm theoretically, this is lower than the expected value. When the negative charge domain dislocated towards the imidazole group, the negative charge interaction is making C12 virtually shielded and as neutral. So, the chemical shift of such carbon becomes below 100 pm. The imidazole group has three carbons C16, C17 and C18, whose chemical shifts are 147.4, 174.29 and 146.94 ppm theoretically, but they are very close between 136-138 ppm experimentally. Among these, C17 is directly connected between two nitrogen atoms, hence it is expected to have higher chemical shift 174.29 ppm theoretically, but this difference is not observed experimentally. This shows the charge distribution in imidazole group is not in accordance with the Mullikan prediction, whereas there is a type of uniform distribution or conjugation happens within the imidazole ring also. But the general increase in the chemical shift value is clearly due to the presence of the N atoms in this ring.

The chemical shifts of the hydrogen atoms in benzene ring are expected between 7-8 ppm. In this case also, for all the hydrogen atoms in the benzene ring, the same range is observed both experimentally and theoretically. Almost the same values are also observed for hydrogen atoms in the imidazole group which shows the charge prediction by Mullikan analysis for hydrogen atoms are correct. Among the ethylene group two hydrogen atoms, the theoretical shift are 3&4 ppm but 5 ppm experimentally for both atoms, this trend is in tune with the above literature. There is no appreciable difference observed in the chemical shifts in different solvents phases.

Hence the impact of the solvents on the chemical shifts of the compound for various atoms is negligibly small.

4.6. Frontier molecular interaction profile

The Frontier molecular interaction chart is displayed in the Figure 7. The HOMO-LUMO energy levels are generally formed by the linear combinations of atomic orbitals. The sum of atomic orbitals is usually equal to the number of molecular orbitals in which the electronic transitions taking place. Normally, the bonding electrons are spending most of their time in between the corresponding nuclei whereas non-bonding electrons spending most of the time away from their nuclei. Thus, the chemical activity of the atoms resulting blended chemical reaction of the molecule and which is also depend upon the bonding electrons. All parts of the atomic orbitals which overlap each other and have same sign (same color). If there are atomic orbitals with same energy (degenerate) between the molecules, they will be combined to form σ and π orbital. The interaction often appeared between the molecular orbitals and leads the asymmetrical delocalization of molecular orbitals. Such a dislocation of electron clouds cause the born of new chemical property for the compound.

In the case of LUMO, the σ-bonding orbitals interaction seems to be there in the benzene ring carbons. The σ-bonding orbitals (empty) are produced diagonally, which means that, the degenerate energy levels are overlapped and form same color. There are two different colors appeared (blue and orange) contradictory which shows the diagonal interactions. But, in the case of HOMO, the π-bonding orbital interaction taking place over the imidazole ring which are made by C=C and C=N bonds. This view in the compound shows that, the filled orbitals found in five membered ring. Thus, first transition is observed between HOMO and LUMO with the band gap of 4.092 eV. This wide energy gap ensures the good stabilization of the compound which explicit the hardness of chemical reactivity. This view of the compound showed that, it will not react with any molecule except corresponding protein receptor.

In HOMO+1, the sigma orbital interaction is started from the benzene ring and ended with C=C and C=N of the imidazole group via CH_2 group. It is very important to infer that, the chemical reaction taking place between two rings and the asymmetrical movement of the electron clouds is the main cause of the compound being antifungal.

4.7. Molecular electrostatic potential (MEP) maps

The molecular electrical potential surfaces from Figure 8 illustrate the charge distributions of molecules three dimensionally. This map allows visualizing variably charged regions of a molecule. The knowledge of the charge distributions can be used to determine how molecules interact with one another and it is also used to determine the nature of the orientation of chemical bond [28-29].The figure shows the negative charges are more concentrated at the top of the imidazole group, whereas the blue region is spread over around the hydrogen atoms of the phenyl ring. The rich negative region (electrophilic) is found to be on imidazole group since the orientation of electron cloud on that side. The opposite region is highly positive (nucleophilic) located on C-H bonds of the ring. The color code of the MEP map is in the range from –.4.98 a.u. (deepest red) to 4.98 a.u. (deepest blue) in the compound. From this observation, it is clear that, the imidazole group is acting as main receptor branch for binding the compound with protein.

4.8. Electronic excitation analysis

The molecular interactions between electron donors and acceptors are generally associated in the formation of intensity colored charge–transfer (CT) complexes which absorb radiation in the UV-Visible region [30-32]. The delocalized electrons in the compound are directly showed the formation of CT complexes which stimulate the biological activity [33]. In this case, the electronic excitation absorption CT band is found at 253 nm with oscillator strength of 0.007 at the energy gap of 4.8 eV and the absorption band is assigned to $n \rightarrow \pi^*$ transition in gas phase. The electronic transition in excited electronic state produces the characterization intense color CT complex. The energy of CT complex is found to be 4.908 eV which is high enough to ensure the transition between acceptor (five membered ring) and donor (six membered ring). In solvent phase, the CT band is identified at 232 nm with oscillator strength of 0.316 at the energy gap of 4.72 eV. The obtained result of the CT complex in ethanol solvent phase showed the strong interaction between donor and acceptor. The CT absorption band is rarely lying in the UV and frequently visible region of the spectrum and naturally being with biological activity. In this case, the absorption band is found at quartz-UV region which infer that, the

formation of imine in imidazole group is the root cause of the antibacterial and antifungal activity. The electronic excitation parameters are presented in the Table 5 and the absorption band is displayed in the Figure 9.

The electronic displacement between the molecular orbitals give rise to Circular Dichroism called ECD which is directed along the orbital interaction helical path, implies a simultaneous translation and rotation of charge. The electron cloud displacement is redistributing charge levels during the transition. Usually, due to the addition of the chromophores in the compound, the electron redistribution taking place among Frontier molecular orbitals. Thus, the electronic orientation alters the chemical activity of the compound which can be identified easily by the ECD. According to the Figure 9, the ECD absorption band is identified at 5.5 eV which directly explicit the rich chemical reactivity supported by imidazole group.

4.8. Chemical parameters

The energies of the HOMO-LUMO, energy gap and different reactivity descriptors of molecule in both optimized and electronic transition levels are presented in Table 6. The ionization potential and electron affinity are found to be 6.430 and 0.88 respectively. The lower and higher degree of above said parameters showed the chemical consistency of the present compound. The electronegativity, which is a measure of asymmetrical dislocation of electron clouds in the compound, has 3.65 and 3.62 eV in optimized and electronic states respectively. This view ensures the asymmetrical dislocation of the charge levels. The chemical hardness of the present compound is 2.77 and 2.73 eV in optimized and transition state respectively, which shows that the present molecule is not easy to react with other compound except protein receptor[34].

The electrophilicity index is a measure of lowering of total energy due to the maximal electron flow between the donors and the acceptors. The electrophilicity indices are 2.41 & 2.39 eV in optimized and transition state respectively, whereas in the case of benzene ring is 2.09 eV. This shows that the electrophilicity index, which is the measure of the lowering of total energy, is increased during transition [31].The dipole moment in a molecule is another important electronic property. The dipole moment of the benzene ring is almost zero, whereas by addition

of the ethyl and imidazole groups, dipole moment of the present molecule is increased by 4.21 and 4.22 Debye in optimized and transition state respectively, which shows the charge flow conventional direction. Here, the ethyl benzene is composed with imidazole group and form the consistent compound where the electrophilicity charge transfer is found to be +0.38 which shows that, the charge flows from imidazole to ethyl benzene while binding. This view indicates that, the chemical property of ethyl benzene is changed on par with imidazole group. This is the major mechanism taking place while binding the present compound being with pharmaceutical potential.

4.9. NBO profile

The Table 7 shows the various possible donors and acceptors in molecule with their occupancy value in each position, similarly the various possible transitions among these donors and acceptors. The stabilization energy for these transitions give a measure of the probabilities of these transitions; which indicate the highly probable in this molecule are C1-C6 to C2- C3 (π -π*, 21.44 Kcal/mol), C2-C3 to C4- C5 (π -π*, 20.31 Kcal/mol), C16-C18 to C17- N22 (π -π*, 15.13 Kcal/mol), C17-N22 to C16- C18 (π -π*, 21.39 Kcal/mol), N15 to C16-C18(n -π*, 30.19 Kcal/mol) and N15 to C17-N22(n -π*, 46.13 Kcal/mol).Of which the most probable transition is n -π* transition from N15 to C17-N22 (n -π*, 46.13 Kcal/mol), and the next probable transitions areN15 to C16-C18 (n -π*, 30.19 Kcal/mol), and C17-N22 to C16- C18 (π -π*, 21.39 Kcal/mol) which takes place within the substitution group.

The probable σ-σ* and π-π* transitions are taking place between different bonds of the benzene ring with maximum energy of 20.31 kcal/mol. but in the case of ethyl group, the transition appeared with minimum energy of 4.58 kcal/mol. the strong π- π* transition is observed between lone pair of N15 to C16 - C18 and C17 - N22 with the dependable energy of 30.19 and 46.13 kcal/mol respectively. These are the highest energy which is utilized for the formation of the important imine group. This is the most significant process which explicit the key property of the compound.

4.10. Polarizability and first order hyperpolarizability analysis

In order to investigate the relationships among molecular structures and polarizability - first

order hyperpolarizability of the compound, the polarization calculation has been carried out and the magnitudes are presented in the Table 8.

The calculated value of the dipole moment is found to be 4.21 Debye. The highest value of the dipole moment is observed for component $\mu_{x,}$ which is equal to 2.45D and the lowest value of the dipole moment of the molecule for the component μ_y is -1.0734 D. The calculated shows the intense orientation of the charge levels in x component of the three axes of the compound which indicate that, the direction of the imidazole group. The calculated average polarizability and anisotropy of the polarizability is $3.025x10^{-24}$esu and $6.7194x10^{-24}$esu, respectively. The hyperpolarizabilityβ is one of the important key factors in frontier molecular orbital interaction system. The B3LYP/6-311+G (d,p) calculated first hyperpolarizability value (β) is 362 $x10^{-33}$esu. From this observation, it is clear that, the hyper asymmetrical polarization is taking place in order to emphasize the formation of imidazole group with peculiar charge orientation support. This observation is further stressed from the obtained dipole moment value which is 3.065.

4.11. Thermodynamical functions analysis

The entropy, specific heat capacity and enthalpy of the crystal compound since they play a important role in physical as well as chemical properties [35]. In this case, the calculated thermodynamic functions are depicted in the Table 9. The coefficients of entropy, specific heat capacity and enthalpy were varied with respect to temperature in positive mode. When the temperature increased from 100K to 1000K, the thermodynamical functions found to vary as linear curve and sustained up to the maximum temperature. This linear variation shows the chemical stability of the present compound was consistent.

Similarly, the Gibbs free energy also has negative temperature coefficient. This negative coefficient established the chemical reaction is uninterrupted. Normally, the chemical reaction is feasibly occurring when the Gibbs free energy of the molecular system decreases. If ΔG is negative or less than zero, the chemical reaction will be constant. In this case, the Gibbs energy is found be varied negatively up to 1000K and it is inferred that, the present compound is chemically strong and react easily with receptor protein with minimum amount of energy.

4.12. VCD analysis

Chirality is a chemical property that is very important to current pharmaceutical development processes. Chirality can be studied using the vibrational optical activity (VOA) of molecules. VOA is the differential response to left versus right circularly polarized infrared radiation during a vibrational transition [36-37]. VCD can be used for many types of analysis related to the structure and conformations of molecules of biological interest; Determining the enantiomeric purity of a sample relative to a known standard, Determination of absolute configurations and Determination of the solution conformations of large and small biological molecules. VCD studies consist of a combination of spectral measurement and electronic structure calculations.

The VCD spectrum of a chiral molecule is dependent on its three-dimensional structure: more specifically, its conformation and absolute configuration. Thus, VCD can allow determining the structure of a chiral molecule. Both the IR and VCD spectra of diasteriomers and for enantiomers, the IR spectra are again identical, but the VCD spectra have opposite sign. The VCD results provided by electronic structure calculations can be used to identify the absolute configuration producing a given observed spectrum, and they can also elucidate the contributions of different conformations to a spectrum.

The VCD spectrum of the title compound is displayed in the Figure 9. If electronic structures of both enantiomers are same, the compound will have no additive properties which may affect the basic function of the chemical compound[38]. In this case, the absolute configuration of both enantiomers is same. From this observation, it can be inferred that, the basic pharmaceutical property of the compound is active and no side effects are produced while consume.

5. Conclusion

By the conformational analysis, the stable conformer with lowest energy is identified and same is used for further analysis. The study of the molecular geometry reveals that there is no appreciable change in the bond length and bond angle of the molecule by addition of the substitutional group.

The C-H observed vibrations indicate that the stretching, in-plane bending and out-of-plane are observed in the expected region, because ethylene group acts as bridge between imidazole and phenyl ring and it is not affected by either sides of the group's vibrations. The stretching vibration of C=N is increased much in the present molecule than the usual trend because of the influence of the phenyl ring whereas C-N has slight variation because of the phenyl ring.

The special property; antiparasitic, antifungal and antimicrobial activities of the compound are investigated from the spectral chemical shift. The interpretation of bio molecular activity is studied from the dislocation of the Frontier molecular orbitals. The NBO analysis ensured the charge transfer between the localized σ and π bond and lone pair orbitals. The activity of electronic excitation energy levels for the potential pharmaceutical activity has been analyzed by calculating E_{CT} and Gibbs free energy.

References

[1] http://www.scbt.com/datasheet -200530-benzyl imidazole html

[2] B Hachula, M Nowak, J Kusz, Crystal and molecular structure analysis of 2-methylimidazole. J chem. Crystallogr (2010) 40: 201-206.

[3] Norman SM, Bennet RD, Poling SM, Maier VP, Nelson MD , Paclobutrazole inhibits abscisic acid biosynthesis incercosporaresicola**,** (1986) Plant Physiol 80:122–125

[4] Purohit M, Srivastava SK (1991) ProcNatlAcadSci IndiaA61:461–466

[5] Khabnadideh S, Rezaei Z, Khalafi-Nezhad A, Bahrinajafi R,Mohamadi R, Farrokhroz AA (2003) Bioorg Med ChemLett13:2863–2865

[6] Wilkinson CF, Hetnarski K (1974) BiochemPharmacol, 23:2377–2387

[7] R. Hofman, Imidazole and its Derivatives, IntersciencePublishers New York, 1953.

[8] M. Manzoor ali, Gene George, S. Ramalingam, S. Periandy, V. Gokulakrishnan, Journal of Molecular Structure 1106 (2016) 37-52.

[9] Barbara Hachuła, Maria Nowak, Joachim Kusz, ,Crystal and Molecular Structure Analysis of 2-Methylimidazole,ChemCrystallogr (2010) 40:201–206

[10] J. MarekWojcik, JacekKwiendaczMarekBoczar,ŁukaszBoda, Yukihiro Ozaki, Quantum mechanical and car-parrinello. Molecular dynamics simulations of infrared spectra of crystalline imidazole Journal of Molecular Structure 1072 (2014) 2–12.

[11] P. Hunt, B. Kirchner and T. Welton, Chem. Eur. J, 2006, Vol 12, Iss 26, 6762-6775.

[12] G. Rauhut, P. Pulay,,Transferable scaling factors for density functional derived. Vibrational force fields, J. Phys. Chem. 99 (1995) 3093-3100.

[13] A.P. Scott, L. Radom, Reported energies include zero-point energy corrections scaled by 0.9806, J. Phys. Chem. 100 (1996) 16502-16513.

[14] Y.R. Sharma, Elementary Organic Spectroscopy, Principles and Chemical Applications, S.Chande& Company Ltd., New Delhi, 1994, 92–93.

[15] P.S. Kalsi, Spectroscopy of Organic Compounds, Wiley Eastern Limited, New Delhi, 1993.

[16] J.L. Duncan, E. Hamilton, An improved general harmonic force field for ethylene, J. Mol. Struct. (Theochem) 76(1981) 65.

[17] R.N. Singh, S.C. Prasad, Spectrochimica Acta A 34 (1974) 39.

[18] Naji A Abood et al, Journal of Science (C) (2012) Vol. 30(1), 119-131.

[19] G. Shakila, S. Periandy, S. Ramalingam, Spectrochimica Acta Part A 78 (2011) 732–739.

[20] P. Bassignana et al., Spectrochimica Acta, (1965), 21, 605-612.

[21] George Socrates, Infrared and Raman Characteristic group frequencies, 3rd ed. Wiley, New York, 2001.

[22] M.Silvestein, F.X. Webster, Spectrometric Identification of Organic Compounds, 6th ed, John willey, Asia, 2003.

[23] L. Colombo, K. Furic and D. Kirin,Dynamics of organic molecular crystalsJounal of Molecular structure, 46(1978)495-501.

[23] Ana. E. Lesdesma et al, Magnetic Resonance Spectroscopy, ISBN 978-953-51-0065-2, 2012.

[24] P. Excoffon and Y.Marechal, H-bonds of imidazole crystals.I. Measurements of polarized light IR spectra, Chemical Physics 52 (1980) 237-243

[25] V. Krishnakumar, S. Manohar, R. Nagalakshmi, Crystal growth and characterization of N-hydroxyphthalimide (C8H5NO3) crystal, SpectrochimicaActa Part A 71 (2008) 110–115.

[26] M. Manzoor ali, Gene George, S. Ramalingam, S. Periandy, V. Gokulakrishnan, Journal of Molecular Structure 1106 (2016) 37-52.

[27] V. Karunakaran, V. Balachandran, Spectrochimica Acta Part A: Molecular and Biomolecular Spectroscopy 128 (2014) 1–14.

[28] C.H. Choi, M. Kertesz, Journal of Chemical Physics, (1998), 108, 6681.

[29] Per. Sjoberg, Peter. Politzer, Journal of Physical Chemistry, (1990), 94 (10), 3959–3961.

[30] R. Foster, Organic Charge -Transfer Complexes, Academic Press, New York, 1969.

[31] E.M. Abd-Alla, A.A.A. Boraei, M.R. Mahmoud, Can. J. Appl. Spectrosc. 39 (1994) 123.

[32] H.S. Bazzi, A. Mostafa, S.Y. AlQaradawi, E.M. Nour, J. Mol. Struct. 842 (2007) 1.

[33] Abdelmajid A. Adam, Moamen S. Refat, T. Sharshar, Z.K. Heiba, Spectrochim. Acta Part A, (2012).

[34] S. Xavier, S. Periandy, Spectrochimica Acta Part A149 (2015) 216–230.

[35] S. Ramalingam, I. John David Ebenezar, C. Ramachandra Raja, P.C. Jobe Prabakar, J Theor. Compu.t Sci. 2014, 1:2.

[36] T. de Boer, G. Maura, M. Raiteri, C. J. de Vos, J. Wieringa, and R. P. Pinder, Neuropharmacology, 27 (1988) 399.

[37] R. K. Dukor and L. A. Nafie, in Encyclopedia of Analytical Chemistry: Instrumentation and Applications, Ed. R. A. Meyers (Wiley, Chichester, 2000) 662-676.

[38] M. Vargek, T. B. Freedman, and L. A. Nafie, J. Raman Spectrosc., 28 (1997) 627.

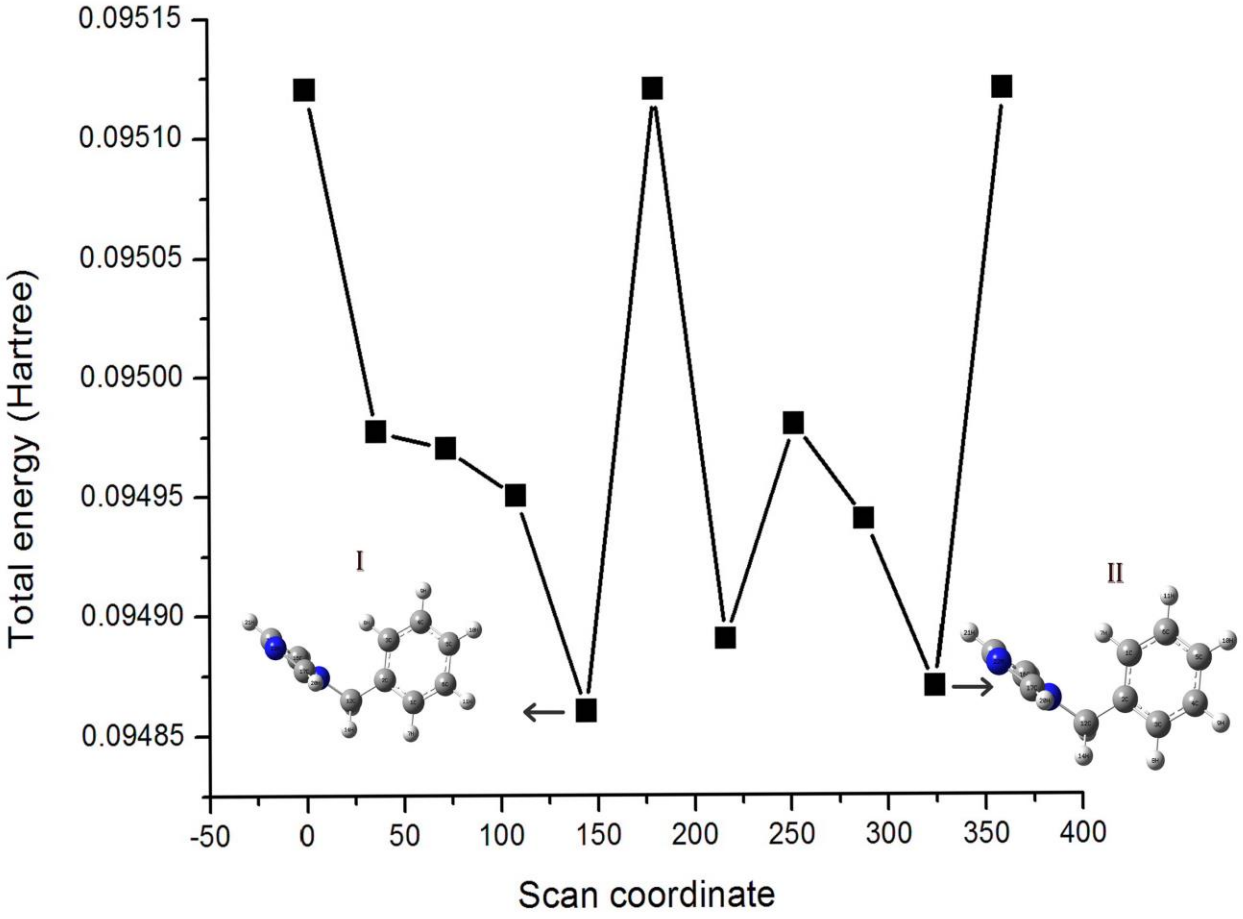

Figure 1: Potential energy graph of 1-Benzylimidazole

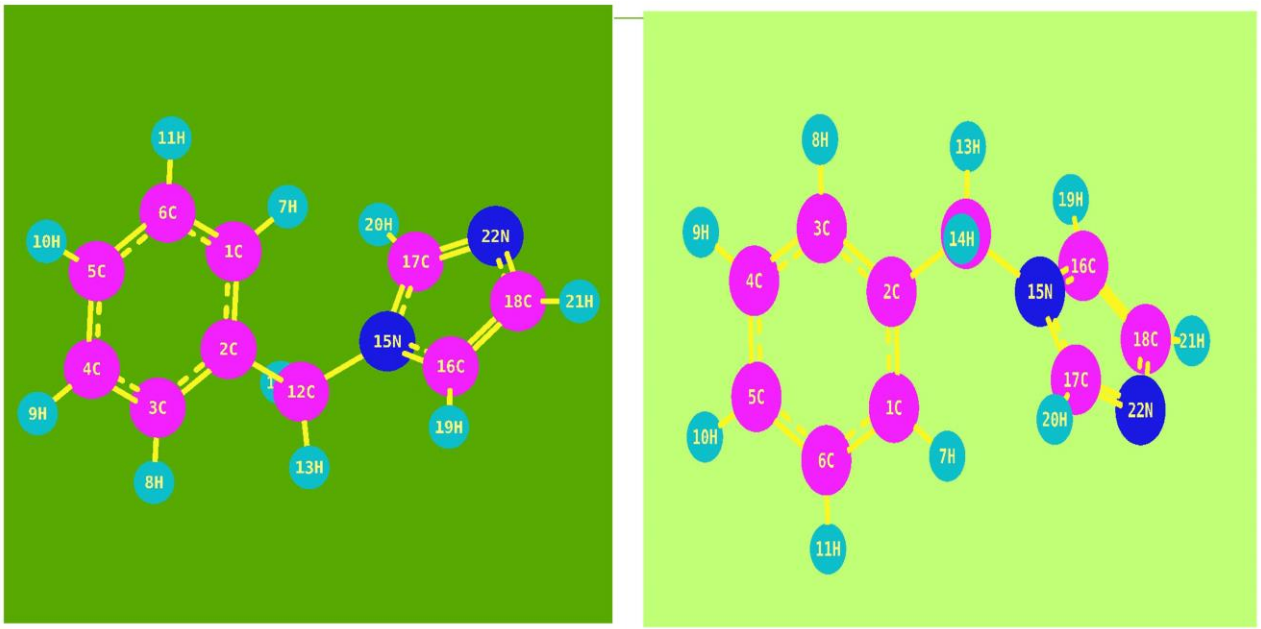

Figure 2: mulliken charge level configuration

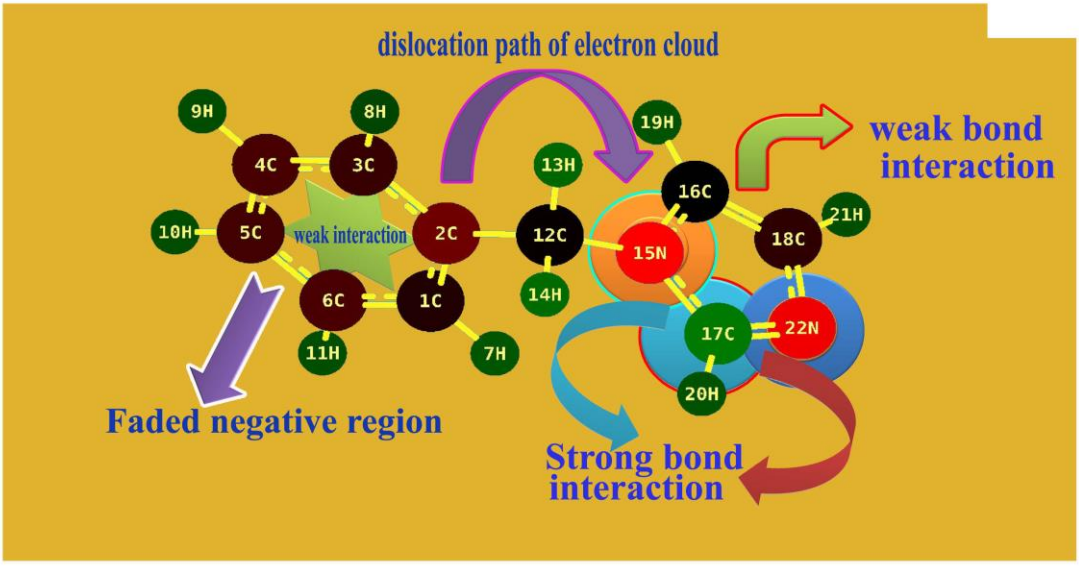

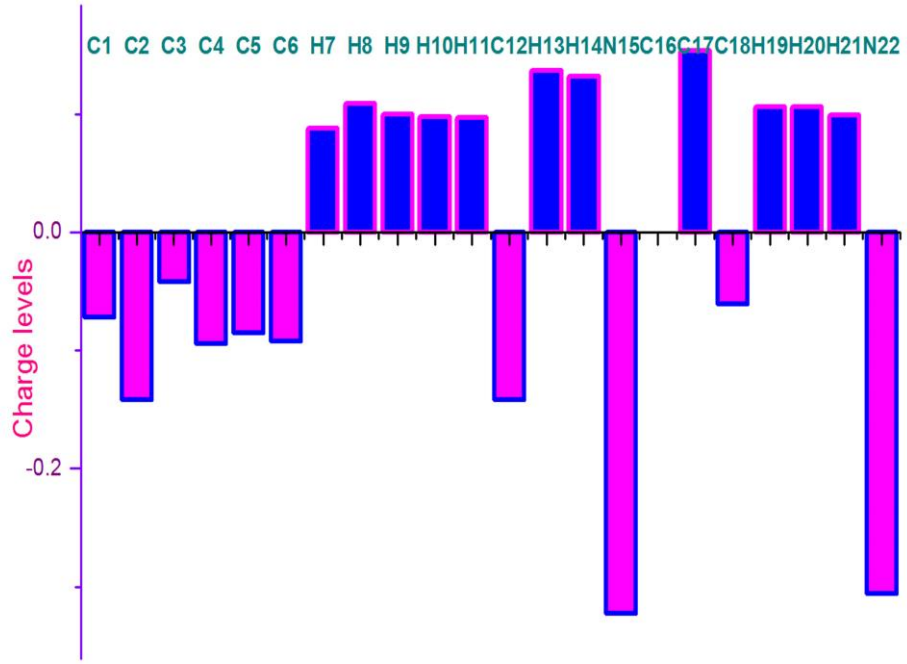

Figure 3: Mulliken charge level diagram

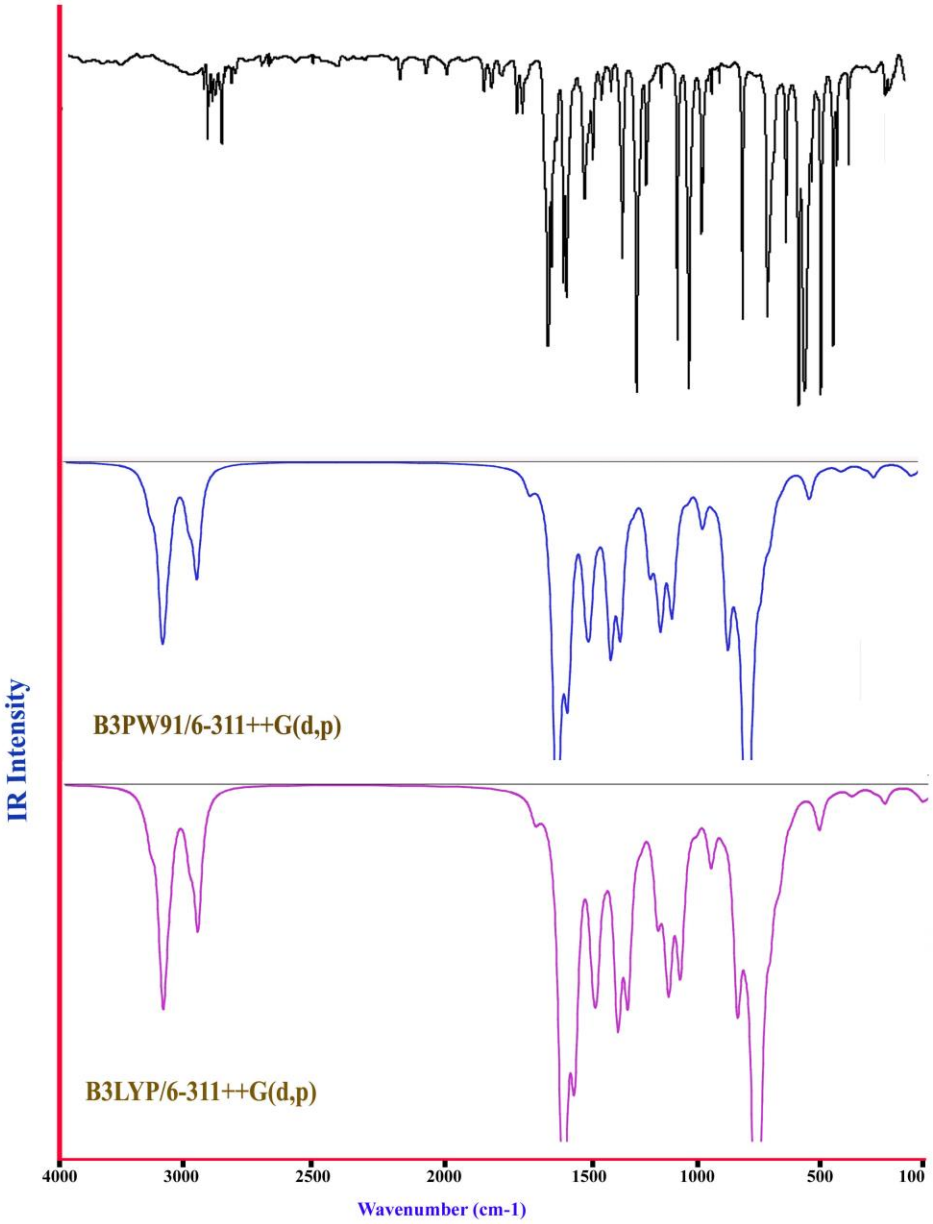

Figure 4: Experimental and calculated FTIR spectra of 1-Benzylimidazole

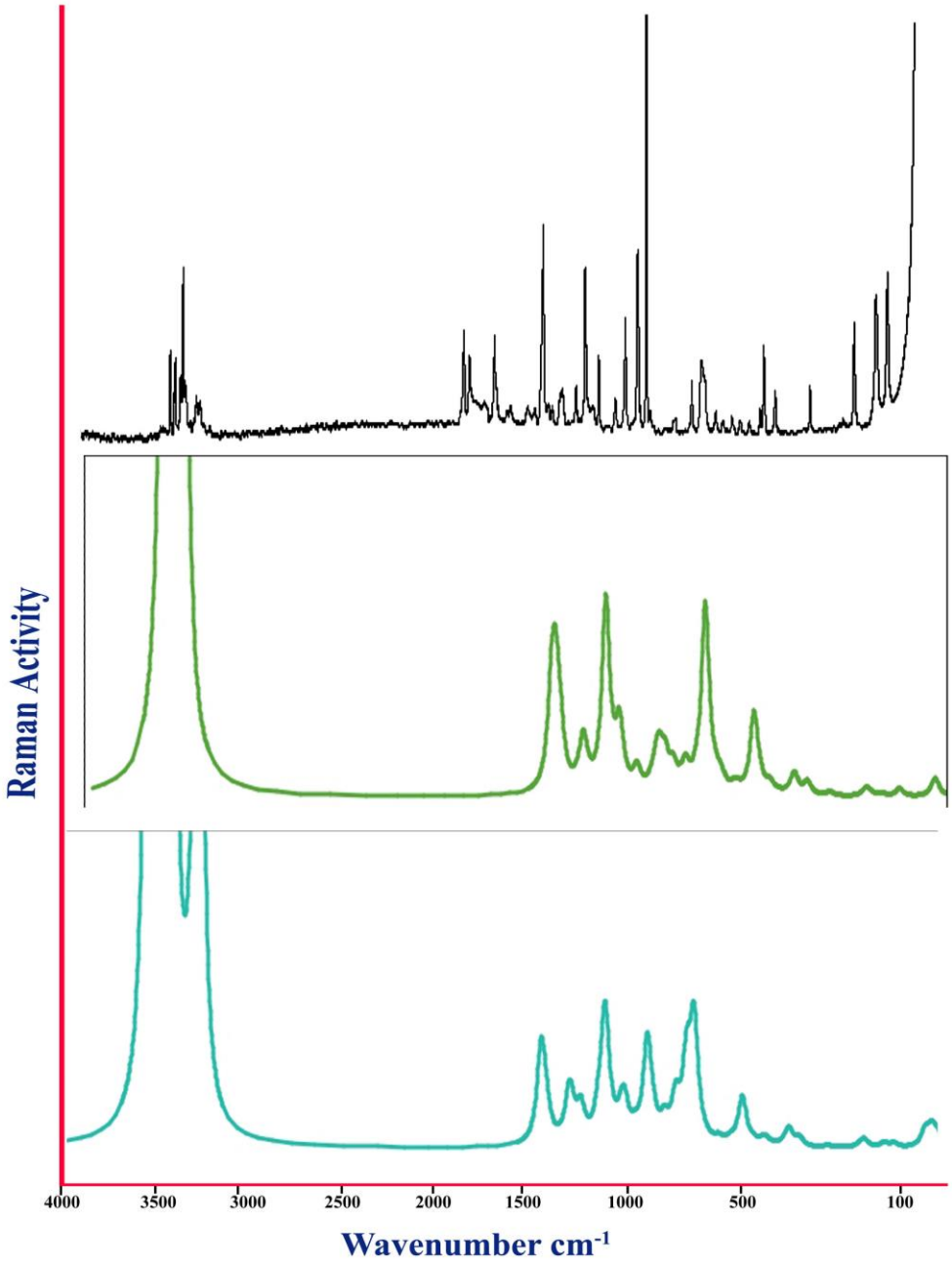

Figure 5: Experimental and Calculated FT-Raman spectra of 1-Benzylimidazole

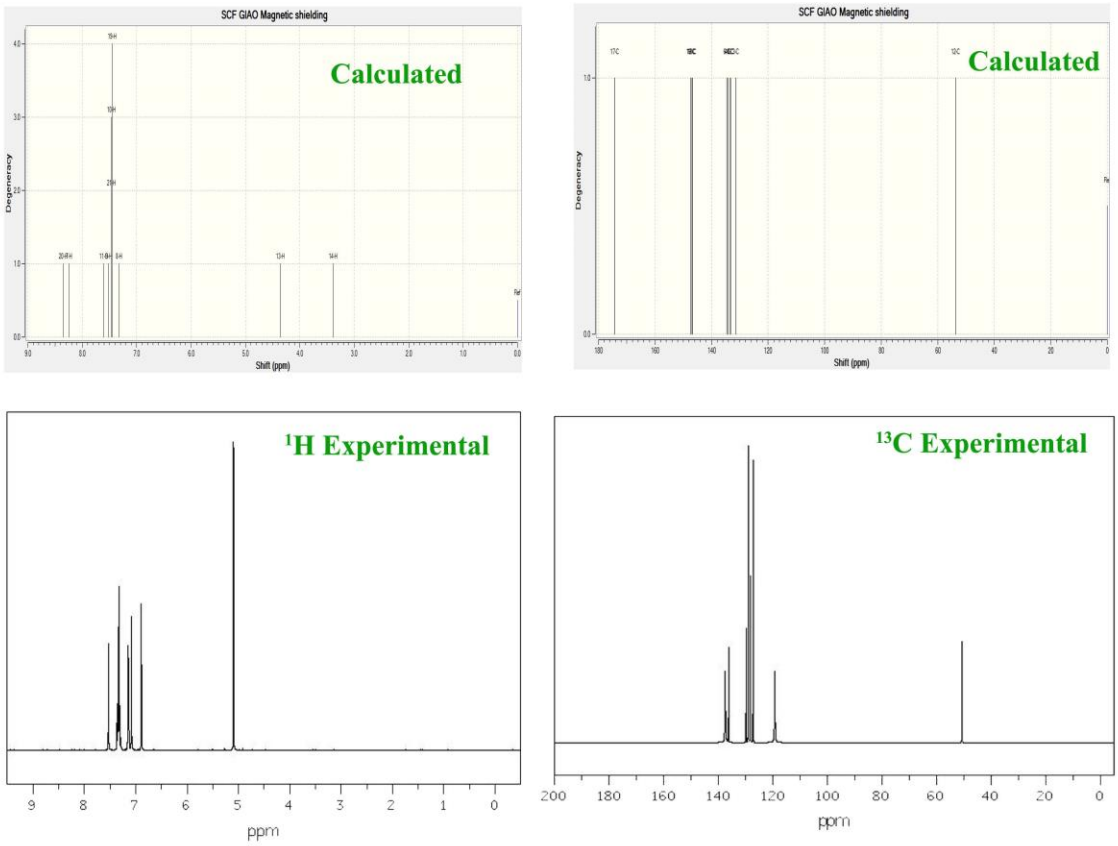

Figure 6: Experimental and calculated ^{1}H and ^{13}C NMR chemical shifts (ppm) of 1-benzylimidazole

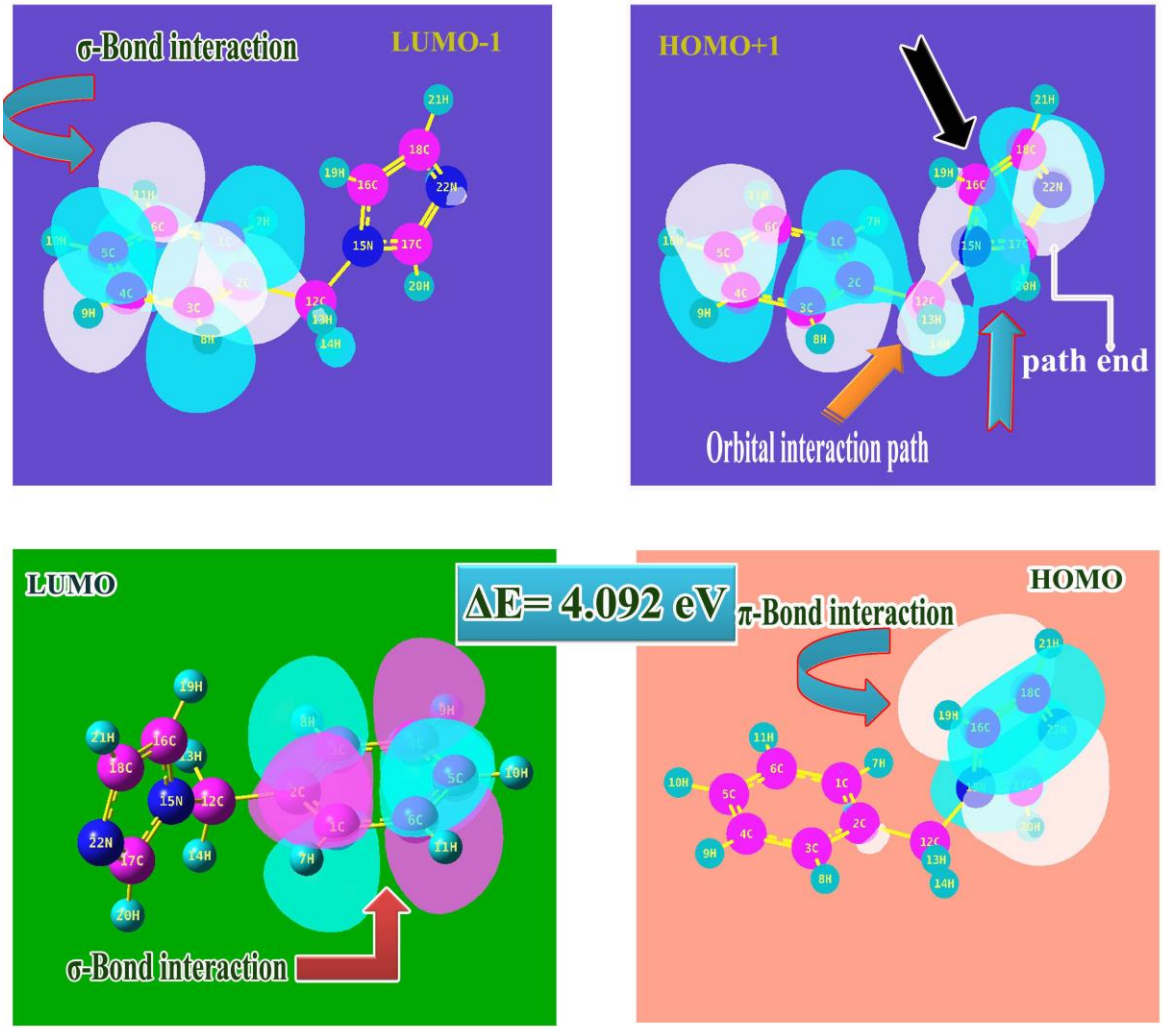

Figure 7: Frontier molecular orbital interaction of 1-Benzylimidazole

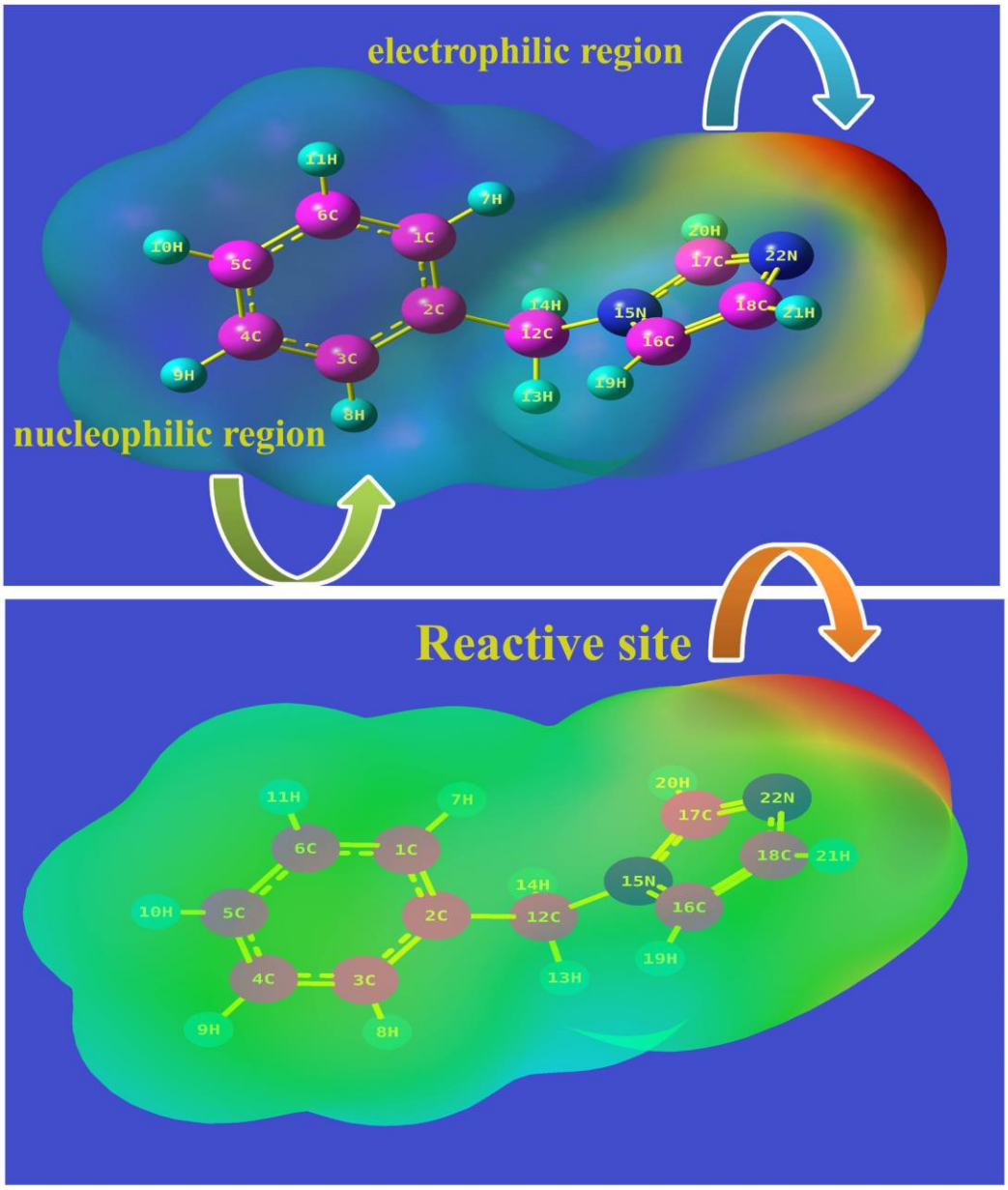

Figure 8: MEP view of 1-Benzylimidazole

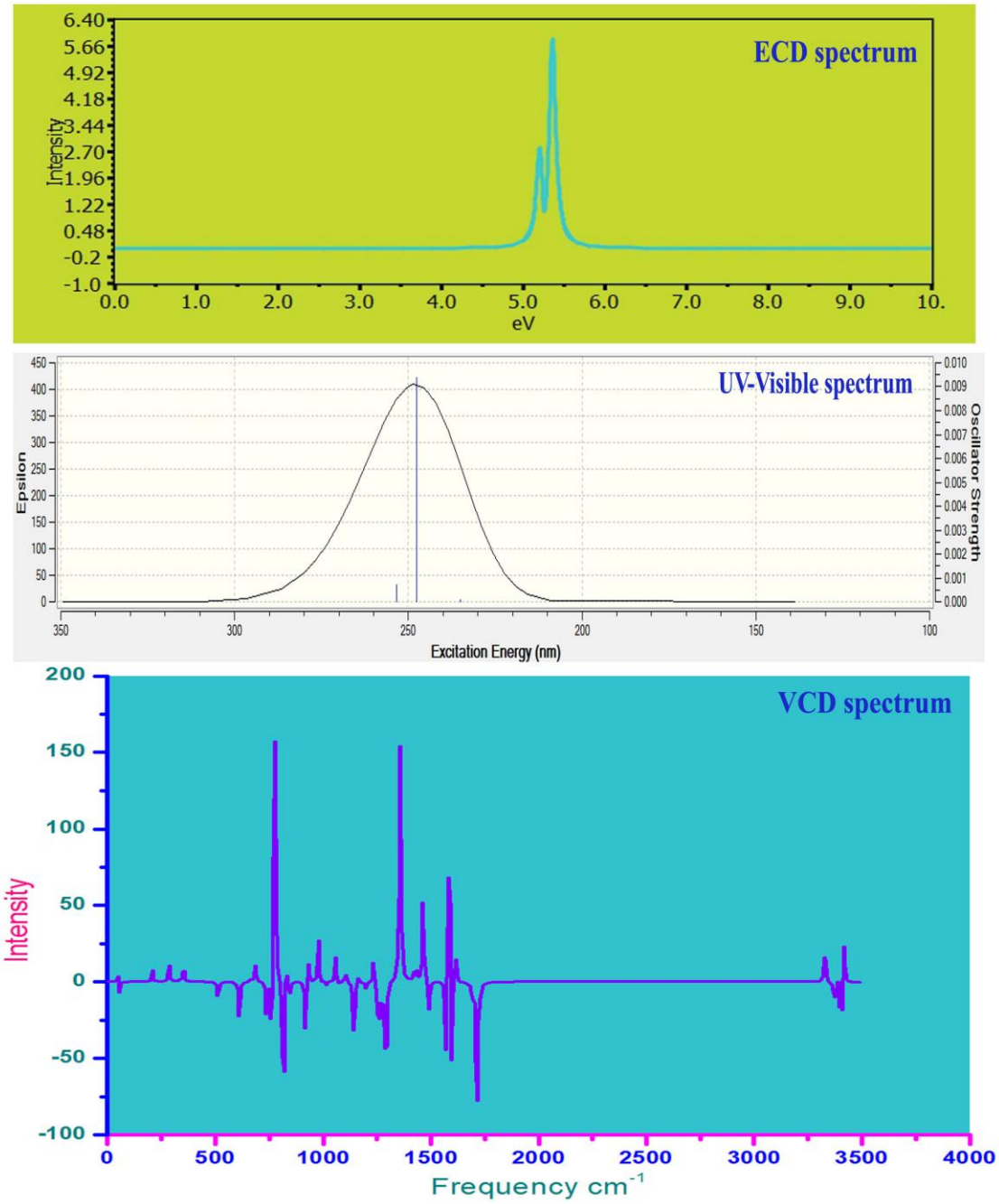

Figure 9: VCD, ECD and UV-Visible spectra of 1-Benzylimidazole

Table 1: The optimized geometrical parameters of 1-Benzylimidazole

Geometrical parameters	B3PW91/6-31+G(d,p)	B3PW91/6-311+G(d,p)	B3LYP/6-311 +G(d,p)	XRD
Bond Length (Å)				
C1-C2	1.398	1.396	1.397	1.394
C1-C6	1.394	1.393	1.392	1.350
C4-C5	1.394	1.085	1.393	1.363
C5-C6	1.395	1.397	1.394	1.375
C2-C3	1.398	1.518	1.396	1.382
C3-C4	1.395	1.391	1.394	1.376
C2-C12	1.515	1.084	1.518	1.510
C16-C18	1.373	1.394	1.371	1.366
C1-H7	1.086	1.084	1.084	0.930
C3-H8	1.088	1.392	1.085	0.930
C4-H9	1.086	1.084	1.084	0.930
C5-H10	1.086	1.084	1.084	0.930
C6-H11	1.086	1.094	1.084	0.930
C12-H13	1.096	1.093	1.093	0.970
C12-H14	1.096	1.457	1.094	0.971
C16-H19	1.079	1.380	1.077	0.930
C17-H20	1.082	1.368	1.080	0.930
C12-N15	1.451	1.370	1.458	1.472
N15-C16	1.377	1.077	1.380	1.471
N15-C17	1.365	1.080	1.368	1.352
C17-N22	1.315	1.312	1.313	1.331

C18-H21	1.081	1.079	1.079	0.930
C18-N22	1.372	1.375	1.375	1.384
Bond Angle (º)				
C2-C1-C6	120.38	120.66	120.41	121.66
C2-C1-H7	119.69	119.66	119.77	119.23
C6-C1-H7	119.93	119.67	119.82	119.21
C1-C2-C3	119.04	118.98	118.99	118.19
C1-C2-C12	121.31	119.81	121.32	121.62
C3-C2-C12	119.62	121.18	119.66	120.18
C2-C3-C4	120.64	120.42	120.67	120.1
C2-C3-H8	119.72	119.70	119.70	119.95
C4-C3-H8	119.65	119.88	119.63	119.91
C3-C4-C5	120.02	120.27	120.02	121.55
C3-C4-H9	119.79	119.69	119.81	119.22
C5-C4-H9	120.19	120.04	120.18	119.23
C4-C5-C6	119.63	119.65	119.63	118.98
C4-C5-H10	120.19	120.17	120.19	120.47
C6-C5-H10	120.18	120.19	120.18	120.56
C1-C6-C5	120.29	120.01	120.28	119.47
C1-C6-H11	119.64	119.81	119.67	119.21
C5-C6-H11	120.07	120.17	120.05	120.27
C2-C12-H13	109.88	110.02	109.78	109.50
C2-C12-H14	109.99	109.72	109.99	109.52
C2-C12-N15	114.18	114.29	114.34	110.54
H13-C12-H14	106.70	106.75	106.77	108.08

H13-C12-N15	109.11	106.62	109.05	109.57
H14-C12-N15	106.67	109.13	106.61	109.04
C12-N15-C16	126.85	126.91	126.91	126.26
C12-N15-C17	126.67	126.76	126.72	124.95
C16-N15-C17	106.48	106.33	106.37	108.23
N15-C16-C18	105.53	105.60	105.65	106.94
N15-C16-H19	121.93	121.85	121.95	126.53
C18-C16-H19	132.53	132.55	132.40	125.92
N15-C17-H20	121.78	121.68	121.79	125.35
N15-C17-N22	112.35	112.35	112.25	109.37
H20-C17-N22	125.87	125.97	125.96	125.28
C16-C18-H21	127.88	127.94	127.96	125.91
C16-C18-N22	110.65	110.65	110.53	108.32
H21-C18-N22	121.47	121.41	121.51	125.77
C17-N22-C18	104.99	105.07	105.19	107.77
Dihedral angle(º)				
C6-C1-C2-C3	-0.2216	0.4852	0.4186	-
C6-C1-C2-C12	177.6372	-177.5399	-177.6149	-
H7-C1-C2-C3	179.0164	-179.3859	-179.4814	-
H7-C1-C2-C12	-3.1247	2.589	2.4852	-
C2-C1-C6-C5	-0.1223	-0.3525	-0.2847	-
C2-C1-C6-C11	179.7545	-179.8676	-179.9084	-
H7-C1-C6-C5	-179.36	179.5187	179.6156	-
H7-C1-C6-C11	0.5168	0.0035	-0.0081	-
C1-C2-C3-C4	0.4396	-0.2572	-0.264	-
C1-C2-C3-C8	-179.3801	179.0351	179.1307	-
C12-C2-C3-C4	-177.4544	177.7397	177.7427	-
C12-C2-C3-H8	2.7258	-2.9679	-2.8626	-
C1-C2-C12-H13	161.8874	98.2451	101.8047	-
C1-C2-C12-H14	-80.8927	-18.916	-15.3897	-
C1-C2-C12-H15	38.9845	-141.8578	-138.242	-
C3-C2-C12-H13	-20.2683	-79.7356	-76.1836	-

C3-C2-C12-H14	96.9516	163.1033	166.622	-
C3-C2-C12-H15	-143.1712	40.1614	43.7697	-
C2-C3-C4-C5	-0.3135	-0.1032	-0.0244	-
C2-C3-C4-C9	-179.8544	179.7695	179.8533	-
H8-C3-C4-C5	179.5064	-179.3943	-179.4198	-
H8-C3-C4-H9	-0.0345	0.4785	0.4579	-
C3-C4-C5-C6	-0.0354	0.2401	0.1625	-
C3-C4-C5-H10	-179.6678	179.8928	179.8783	-
H9-C4-C5-C6	179.5038	-179.6322	-179.7147	-
C12-N15-C16-H19	-0.5842	0.0205	0.001	-
H9-C4-C5-H10	-0.1286	-0.0138	-0.0094	-
C4-C5-C6-C1	0.2519	179.4996	179.6127	-
C4-C5-C6-C11	-179.6245	-179.6664	-179.7249	-
C10-C5-C6-C1	179.8844	-0.153	-0.1028	-
C10-C5-C6-C11	0.008	64.9904	62.8862	-
C2-C12-N15-C16	65.3574	-115.5431	-119.5344	-
C2-C12-N15-C17	-114.5248	-173.224	-175.5397	-
H13-C12-N15-C16	-57.937	6.2425	2.0397	-
H13-C12-H15-C17	122.1809	-58.2693	-60.1593	-
H14-C12-H15-C16	-172.8796	121.1972	117.4201	-
H14-C12-H15-C17	7.2383	179.5339	178.1576	-
C12-H15-C16-C18	-179.9464	-1.1596	-2.511	-
C17-N15-C16-H18	-0.0448	-0.0207	0.1736	-
C17-N15-C16-H19	179.3173	179.2858	179.505	-
C12-N15-C17-H20	-0.3874	0.0813	1.6492	-
C12-N15-C17-N22	179.9279	-179.5573	-178.2442	-
C16-N15-C17-H20	179.7108	179.6368	179.6434	-
C16-N15-C17-H22	0.0261	-0.0018	-0.2501	-
N15-C16-H18-H21	-179.8806	-179.9341	179.856	-
N15-C16-H18-H22	0.0496	0.0361	-0.0535	-
H19-C16-H18-H21	0.8522	0.8655	0.6185	-
H19-C16-H18-H22	-179.2177	-179.1643	-179.2911	-
N15-C17-H22-H18	0.0043	0.0234	0.2132	-

Table 2: Mullikan atomic charge distribution of 1- benzylimidazole

Atoms	B3LYP/ 6-311++G(d,p)
C1	-0.072
C2	-0.142
C3	-0.042
C4	-0.094
C5	-0.085
C6	-0.092
H7	0.088
H8	0.109
H9	0.100
H10	0.098
H11	0.097
C12	-0.142
H13	0.137
H14	0.132
N15	-0.323
C16	0.000
C17	0.154
C18	-0.061
H19	0.106
H20	0.106
H21	0.099
N22	-0.306

Table 3: Observed and computed (scaled) wavenumbers of 1-benzylimidozole

C_s Symmetry species	Observed frequency		Calculated frequency			Vibrational assignments	PED assignments
			B3LYP	B3PW91			
	FT-IR	FT-Raman	6-311++G (d,p)	6-31++G(d,p)	6-311++G(d,p)		
A'	3100m	3100w	3089	3144	3129	**(C-H) υ**	υ(C-H) - 92%
A'	3095m	-	3084	3116	3103	**(C-H) υ**	υ(C-H) - 81%
A'	3090m	-	3071	3110	3098	**(C-H) υ**	υ(C-H) - 95%
A'	-	3080m	3071	3077	3061	**(C-H) υ**	υ(C-H) - 91%
A'	3070w	-	3066	3068	3053	**(C-H) υ**	ν(C-H) - 95%
A'	3060m	-	3060	3060	3045	**(C-H) υ**	υ(C-H) - 100%
A'	-	3050m	3055	3053	3038	**(C-H) υ**	υ(C-H) - 97%
A'	3000m	-	3050	3043	3027	**(C-H) υ**	ν(C-H) - 97%
A'	-	2950w	3049	2973	2958	**(C-H) υ**	υ(C-H) - 99%
A'	-	2900w	3002	2938	2919	**(C-H) υ**	υ(C-H) - 99%
A'	1640s	-	1681	1691	1697	**(C=N) υ**	υ(C-N)+ υ(CC) - 65%
A'	-	1620m	1674	1673	1680	**(C=C) υ**	υ(C-C) +ν(NC) -78%

A'	1610w	-	1663	1590	1599	**(C=C) υ**	υ(C-C)+ δ (HCC) - 44%
A'	1520s	-	1590	1579	1590	**(C=C) υ**	υ(C-C)+ δ (CCC) - 43%
A'	1510s	-	1581	1573	1581	**(C=C) υ**	υ(C-C)+ δ (HCC) - 32%
A'	1460s	-	1562	1535	1543	**(C-N) υ**	δ (CCC) - 55%
A'	1440s	-	1557	1526	1533	**(C-N) υ**	υ(C-C)+ δ (CCC) - 37%
A'	1430s	-	1459	1476	1489	**(C-N) υ**	υ(C-N)+ υ(C-C) 61%
A'	1410m	-	1437	1461	1472	**(C-N) υ**	υ(N-C)+ δ (HCC)- 73%
A'	1380w	-	1423	1444	1456	**(C-C) υ**	υ(C-N)+ υ(C-C)-45%
A'	1350w	1350m	1412	1423	1437	**(C-C) υ**	υ(C-C)+δ (CCN)-70%
A'	-	1340m	1371	1389	1399	**(C-C) υ**	υ(C-N)+ υ(C-C)-64%
A'	-	1320m	1360	1377	1389	**(C-C) υ**	δ (CCN) +(CCCN) - 60%
A'	1290s	-	1323	1259	1317	**(C-H) δ**	δ (HCC) - 57%
A'	1280s	-	1307	1220	1277	**(C-H) δ**	δ (HCC)+ υ(C-C) - 69%
A'	1260s	-	1301	1213	1270	**(C-H) δ**	δ (HCC) - 49%
A'	1210m	-	1285	1202	1261	**(C-H) δ**	δ (HCC)+ υ(C-C) - 86%
A'	1200m	-	1226	1185	1245	**(C-H) δ**	δ (HCC) - 49%
A'	1130s	-	1217	1159	1222	**(C-H) δ**	δ (HCC) +υ(C-C) - 80%

A'	1120s	-	1184	1123	1186	**(C-H) δ**	δ (HCN)+υ(NC)- 66%
A'	1110s	-	1177	1108	1174	**(C-H) δ**	δ (HCC)+υ(NC) - 66%
A'	1090s	-	1160	1074	1141	**(C-H) δ**	δ (HCC)+υ(NC) - 71%
A'	1080s	-	1113	1070	1135	**(C-H) δ**	δ (HCC)+υ(NC) - 74%
A'	1070s	-	1104	1041	1106	**(C=N-C) δ**	δ (CCN) υ(NC)- 53%
A'	1050s	-	1095	1032	1098	**(C-N-C) δ**	δ (CCC)+υ(C-C) - 65%
A'	1040m	-	1060	1016	1082	**(C-N-C) δ**	δ (CCC)+υ(C-C) - 67%
A'	-	1020m	1033	1009	1078	**(C-N-C) δ**	δ (CCC)+ δ(CNCC) - 34%
A'	-	1010m	1028	953	1025	**(C-C-N) δ**	δ (CCC)+υ(C-C) - 59%
A'	-	1000s	1010	952	1023	**(C-C-N) δ**	δ (CCC)+υ(C-C) - 52%
A'		990s	1001	916	988	**(C-C-N) δ**	δ (CNC)+ν(NC) - 80%
A'	920s	-	972	903	979	**(C-C) δ**	δ (CNC)+ν(NC) - 67%
A''	910s	-	964	872	950	**(C-H) γ**	δ (CCCH)+ δ (CNC) 75%
A''	-	850s	954	863	940	**(C-H) γ**	δ (HCCC)+δ(CCCH) - 86%
A''	-	820s	910	831	912	**(C-H) γ**	δ (HCCH) +δ (CNC) - 69%
A''	-	780s	886	797	878	**(C-H) γ**	δ (HCCH)+δ (CNC) - 79%
A''	-	760m	857	793	877	**(C-H) γ**	δ (HCCC) +δ(CCCH) - 78%

A''	-	740s	838	771	854	**(C-H) γ**	δ (CCNH)+ δ(HCCH) - 86%
A''	720w	-	833	742	828	**(C-H) γ**	δ (CNNH) - 83%
A''	-	700s	818	713	801	**(C-H) γ**	δ (HCCH)+ δ(CCNH) - 93%
A''	690w	-	780	700	789	**(C-H) γ**	δ (CCNH)+ δ(HCC) - 59%
A''	-	660s	776	663	754	**(C-H) γ**	δ (CCNH)+ δ (HCC)- 69%
A'	-	650s	663	562	660	**(CCC) δ**	δ (CNCC)+ δ(CCCC)) - 87%
A'	-	610s	621	511	614	**(CCC) δ**	δ (CCCC)+ δ (HCC) - 86%
A'	590m	-	549	447	555	**(CCC) δ**	δ (CCCN) - 92%
A''	480m	-	514	435	543	**(CCN) γ**	δ (CCCC)+ δ (CCN)- 75%
A''	-	340m	444	362	474	**(CNC) γ**	δ (CCCC)+ ν(NC) - 76%
A''	-	250m	418	327	442	**(CNC) γ**	δ (CCCC)+ δ(CCCN) - 77%
A''	-	220m	382	216	338	**(CCC) γ**	δ (NCNC) - 93%
A''	-	180w	346	193	316	**(CCC) γ**	δ (CCNC) - 86%
A''	-	150w	309	175	300	**τ -Ring**	δ (CCCN)+ δ (CCN)- 81%

Table.4: Experimental and calculated ^{1}H and ^{13}C NMR chemical shifts (ppm) of 1-benzylimidazole

Atom	^{1}HNMR			Atom	^{13}CNMR		
	Experimental	computed (B3LYP)			Experimental	computed (B3LYP)	
		Gas	DMSO			Gas	DMSO
7H	7.33	8.24	8.22	**1C**	127.26	133	133
8H	7.33	7.32	7.53	**2C**	136.24	146	147
9H	7.33	7.51	7.66	**3C**	119.26	131	132
10H	7.08	7.47	7.58	**4C**	127.26	133	134
11H	7.14	7.60	7.70	**5C**	128.95	133	133
13H	6.89	4.32	4.54	**6C**	129.80	134	134
14H	5.08	3.38	3.53	**12C**	50.72	53	53
19H	7.08	7.46	7.82	**16C**	136.24	147	150
20H	7.53	8.35	8.48	**17C**	137.43	174	176
21H	7.14	7.46	7.5	**18C**	136.24	146	145

Table 5: Theoretical electronic absorption spectra of 1-benzylimidazole using TD-DFT/B3LYP/6-311++G(d,p) method

λ (nm)	E (eV)	(*f*)	Major contribution	Assignment	Region	Bands
Gas						
253.35	4.893	0.007	H→L (98%)	n→ π*	Quartz UV	R-band (German, radikalartig)
247.66	5.006	0.0094	H→L+1 (97%)	n→π*		
234.97	5.276	0.0001	H-1→L+1 (92%)	π→π*		
DMSO						
237.87	5.212	0.0013	H→L (93%)	n→ π*	Quartz UV	R-band (German, radikalartig)
235.84	5.257	0.0042	H-1→L (79%)	n→π*		
231.13	5.364	0.0088	H-2→L (57%), H-3→L (40%)	π→π*		
Ethanol						
236.14	3.69	0.0111	H→L (86%)	n→ π*	Quartz UV	R-band (German, radikalartig)
232.93	4.72	0.3169	H-1→L (82%)	n→π*		
226.37	5.25	0.0117	H-3→L (48%), H-2→L (47%)	π→π*		

H: HOMO; L: LUMO

Table 6: Chemical parameters of 1-benzylimidazole

Parameters	1-Benzylimidazole			Electrophilicity charge transfer (ECT)
	Optimized state	Excited State by TD-SCF		
		gas	ethanol	$(\Delta N_{max})_A$-$(\Delta N_{max})_B$
HOMO (eV)	6.432	6.359	6.612	
LUMO (eV)	0.882	0.882	0.747	+0.38
Kubo gap (eV)	5.550	5.478	5.864	
Ionization potential (IP)	6.430	6.350	6.610	
Electron affinity E_I	0.88	0.88	0.74	
Electronegativity (eV)	3.657	3.620	3.680	
Global hardness (eV)	2.775	2.739	2.932	
Global softness (eV)	0.360	0.365	0.341	
Electrophilicity Index	2.410	2.393	2.309	
Dipole moment (Debye)	4.21	4.22	5.416	
Charge transfer E_{CT}	-	4.908		

A: Ethyl Benzene: B-Imidazole

Table 7: Second order Perturbation theory of Fock matrix in NBO basis of 1-benzylimidozole

Type	Donor(i)	Occupancy ED/e	Acceptor(j)	ED/e	Energy E(2) kcal/mol	Energy difference E(j)-E(i) a.u.	Polarized energy F(i,j) a.u.
			C1 - C6	0.015	3.11	1.28	0.057
			C2 - C3	0.022	3.69	1.27	0.061
σ- σ*	C1 - C2	1.97288	C3 - H8	0.015	2.53	1.12	0.048
			C6 - H11	0.0137	2.18	1.13	0.045
σ- σ*	C1 - C6		C1 - C2	0.0244	3.52	1.28	0.060
			C2 - C12	0.0287	3.77	1.10	0.057
			C5 - C6	0.0162	2.67	1.28	0.052
		1.97796	C5 - H10	0.0138	2.41	1.13	0.047
π- π*	C1 - C6		C2 - C3	0.3548	21.44	0.28	0.070
		1.66229	C4 - C5	0.3269	20.13	0.28	0.067
σ- σ*	C1 - H7		C2 - C3	0.0222	4.58	1.09	0.063
		1.97857	C5 - C6	0.0162	3.63	1.09	0.056
σ- σ*	C2 - C3		C1 - C2	0.0244	3.69	1.28	0.061
		1.97372	C1 - H7	0.0147	2.48	1.14	0.048

			C3 - C4	0.0152	3.07	1.28	0.056
			C4 - H9	0.0136	2.16	1.13	0.044
π- π*	C2 - C3		C1 - C6	0.3183	19.54	0.29	0.067
			C4 - C5	0.3269	20.31	0.29	0.068
			C12 - H14	0.0155	3.38	0.63	0.045
		1.66565	C12 - N15	0.0297	2.26	0.59	0.035
σ- σ*	C2 - C12		C1 - C6	0.0151	2.30	1.22	0.047
		1.97536	C3 - C4	0.0152	2.33	1.22	0.048
σ- σ*	C3 - C4		C2 - C3	0.0222	3.49	1.28	0.060
			C2 - C12	0.0287	3.70	1.10	0.057
			C4 - C5	0.0161	2.68	1.28	0.052
		1.97796	C5 - H10	0.0138	2.44	1.14	0.047
σ- σ*	C3 - H8		C1 - C2	0.0244	4.54	1.10	0.063
		1.97944	C4 - C5	0.0161	3.56	1.10	0.056
σ- σ*	C4 - C5	1.97937	C3 - C4	0.0152	2.74	1.28	0.053
			C3 - H8	0.015	2.58	1.13	0.048
			C5 - C6	0.0162	2.66	1.28	0.052
			C6 - H11	0.0137	2.48	1.14	0.047

π- π*	C4 - C5	1.66307	C1 - C6	0.3183	20.22	0.28	0.068
			C2 - C3	0.3548	20.19	0.28	0.068
σ- σ*	C4 - H9	1.98006	C2 - C3	0.0222	3.70	1.10	0.057
			C5 - C6	0.0162	3.63	1.10	0.056
σ- σ*	C5 - C6	1.9796	C1 - C6	0.0151	2.72	1.28	0.053
			C1 - H7	0.0147	2.51	1.14	0.048
			C4 - C5	0.0161	2.67	1.28	0.052
			C4 - H9	0.0136	2.53	1.13	0.048
σ- σ*	C6 - H11	1.98006	C1 - C2	0.0244	3.73	1.09	0.057
			C4 - C5	0.0161	3.65	1.10	0.057
σ- σ*	C12 - H13	1.97822	C1 - C2	0.0244	4.00	1.10	0.059
			N15 - C17	0.0395	2.21	0.98	0.042
σ- σ*	C12 - H14	1.97016	C2 - C3	0.3548	4.05	0.55	0.046
			N15 - C16	0.0234	4.90	0.97	0.062
σ- σ*	N15 - C16	1.98196	N15 - C17	0.0395	2.03	1.25	0.045
			C17 - H20	0.0219	2.64	1.20	0.050
			C18 - H21	0.0172	2.90	1.23	0.053
σ- σ*	N15 - C17	1.98641	C16 - H19	0.0122	2.59	1.24	0.051

	C16 - C18	1.9838	C12 - N15	0.0297	5.59	1.03	0.068
π- π*	C16 - C18	1.85539	C17 - N22	0.3827	15.13	0.27	0.061
σ- σ*	C16 - H19	1.98545	N15 - C17	0.0395	2.78	1.01	0.048
			C18 - N22	0.0109	2.85	1.05	0.049
σ- σ*	C17 - N22	1.98432	C12 - N15	0.0297	3.63	1.15	0.058
			C18 - H21	0.0172	3.35	1.26	0.058
π- π*	C17 - N22	1.86833	C16 - C18	0.2979	21.39	0.33	0.078
σ- σ*	C18 - H21	1.9859	C17 - N22	0.0084	2.47	1.10	0.047
σ- σ*	C18 - N22	1.97754	C16 - H19	0.0122	3.32	1.18	0.056
			C17 - H20	0.0219	5.37	1.16	0.070
σ- σ*	N15	1.56028	C2 - C12	0.0287	4.82	0.66	0.056
σ- σ*			C12 - H13	0.0171	4.64	0.63	0.054
π- π*	N15		C16 - C18	0.2979	30.19	0.29	0.087
			C17 - N22	0.3827	46.13	0.28	0.102
σ- σ*	N22	1.92288	N15 - C17	0.0395	7.46	0.81	0.070
			C16 - C18	0.0180	5.09	0.95	0.063

Table 8: The dipole moments μ (D), the polarizability α(a.u.), the average Polarizability α_o (esu), the anisotropy of the Polarizability Δα (esu), and the first hyperpolarizability β(esu) of the compound; 1-benzylimidazole

parameter	Calculated at B3LYP/6-31++G(d,p)	Parameter	Calculated at B3LYP/6-31++G(d,p)
α_{xx}	-1.0288 x 10^{-23}	β_{xxx}	-3.78989 x10^{-32}
α_{xy}	1.24386 x 10^{-24}	β_{xxy}	-9.72077 x10^{-32}
α_{yy}	-1.02451 x 10^{-23}	β_{xyy}	-4.59403 x10^{-32}
α_{xz}	-1.07107 x 10^{-24}	β_{yyy}	6.84077 x10^{-32}
α_{yz}	3.78281 x 10^{-25}	β_{xxz}	1.42713 x10^{-31}
α_{zz}	-1.10653 x 10^{-23}	β_{xyz}	5.07775 x10^{-32}
α_{tot}	-1.05328 x 10^{-23}	β_{yyz}	-3.61727 x10^{-32}
Δα	3.02521 x 10^{-24}	β_{xzz}	-5.77071 x10^{-32}
μ_x	-1.7479 Debye	β_{yzz}	-7.8914 x10^{-32}
μ_y	2.4568 Debye	β_{zzz}	3.62251 x10^{-31}
μ_z	-1.0734 Debye	β	-3.78989 x10^{-32}

Table 9: Thermodynamic properties at different temperatures

T (K)	S_m^0 (cal mol^{-1} K^{-1})	$C_{p,m}^0$ (cal mol^{-1} K^{-1})	ΔH_m^0 (kcal mol^{-1})	**Gibbs free energy** $\Delta G = \Delta H - T\Delta S$ **KJmol^{-1}**
100	307.58	70.03	5.46	-30752.5
200	367.13	109.31	14.27	-73411.7
298.15	420.45	162.76	27.55	-125330
300	421.46	163.83	27.86	-126410
400	476.34	219.49	47.06	-190489
500	530.62	267.30	71.48	-265239
600	582.91	305.99	100.22	-349646
700	632.50	337.12	132.43	-442618
800	679.23	362.50	167.45	-543217
900	723.18	383.53	204.78	-650657
1000	764.52	401.17	244.04	-764276